LIGHT ATTENUATION MODEL TO PREDICT NOMINAL POWER OF MODULES WITH LIGHT-SCATTERING CERAMIC PRINTED FRONT GLASSES

Christoph Kutter, Helen Rose Wilson, Andrea Pfreundt, Martin Heinrich, Harry Wirth
Fraunhofer Institute for Solar Energy Systems ISE, Heidenhofstraße 2, 79110 Freiburg, Germany
christoph.kutter@ise.fraunhofer.de

ABSTRACT: One feasible design for Building-Integrated Photovoltaic modules applies ceramic printed glass covers. Power prediction of such modules is difficult as transmittance of printed glass panes in air was shown to be much lower than the relative power loss in the respective modules for the same print coverage ratio. Applying a matrix-based approach, we developed a light attenuation model, which can describe the relative transmittance decrease of glass panes in air and relative power decrease of modules for glass covers with arbitrary coverage ratios. The model shows good correlation with measured data. The modelled transmittance of glass panes deviate with a root mean square error of 0.55% from the measured transmittance values. The model can compute the module performance loss for investigated coverage ratios with a RMSE of 0.73%.

Keywords: ceramic printed glass cover, enamel, transmittance, PV, BIPV, matrix model, light scattering

1 INTRODUCTION

Ceramic printed glass covers are one design option for Building-Integrated Photovoltaic (BIPV) modules [1, 2]. The print pattern on position 2 of the glass pane in Figure 1 obscures the appearance of silicon solar cells and creates a homogeneous, aesthetic appearance that can satisfy the expectations of architectural design with a prototype shown in Figure 2.
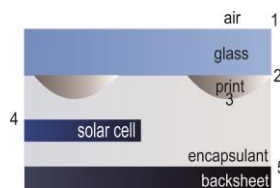
Figure 1: Schematic drawing of module stack with ceramic printed glass cover, print on internal position 2 (not to scale)
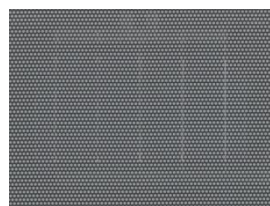
Figure 2: PV module prototype with digitally printed glass cover and blackened connectors

To promote this design approach in industrial manufacturing, understanding of the correlation between print coverage ratio and module performance is crucial.

Frontini *et al.* performed indoor and outdoor tests to evaluate the influence of digital prints on module performance [3]. These authors attested the digitally printed patterns a general technical feasibility for PV applications and found daily yield losses from 10% (white prints), through 15% for green prints, to 35% for black prints with 30% coverage ratio compared to an unprinted reference module.

Mittag *et al.* reported that the measured output power of a laminated PV module is higher than predicted from normal-hemispherical transmittance measurements of the glass pane in air [4]. Due to the large refractive index gap between glass and air, much of this diffuse light is trapped inside the glass pane by total internal reflection. After multiple reflections, all light has been either transmitted, reflected, absorbed or laterally lost through the edges of the pane. The measured normal-hemispherical transmittance of a glass pane in air is lower than in the laminated case for two main reasons. One of these is lateral losses, which can be minimized by an appropriate measurement configuration, as described in [5].The second and more fundamental reason for the difference is that once the glass pane is optically coupled by encapsulant within the module stack, reflection at the glass rear surface is strongly reduced, allowing large fractions of the scattered light to reach the solar cell, explaining the lower module power loss. Mittag *et al.* conclude that neither the hemispherical transmittance of glass panes nor the print coverage ratio qualify as sole indicators to predict module performance within a module efficiency analysis.

Within this paper we present an optical model to calculate the module power decrease with ceramic printed glass. We use a simplified version of the matrix model applied in OPTOS [6] to compute the relative decrease in transmittance of glass panes and relative decrease in performance of modules with arbitrary coverage ratios compared to an unprinted reference. The model requires only a single adjustable parameter, the "print transmittance factor", to describe print coatings.

2 OPTICAL PRINT CHARACTERIZATION

To assess the light scattering, we perform normal, diffuse transmittance measurements on whole-area printed glass panes at the TestLab Solar Facades of Fraunhofer ISE. We find that ceramic prints predominantly transmit diffuse light as shown in Figure 3. The light-scattering characteristics is primarily caused by the composition of the enamel and not by surface roughness or the geometry of the printed pattern. Prints are enamels, which consist of a glass matrix filled with scattering pigments giving an opaque appearance. [5].
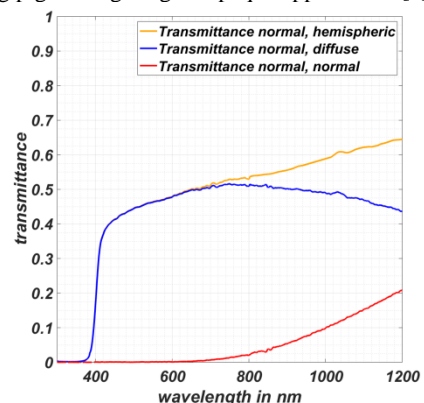
Figure 3: The transmittance of a 100% printed, low-Fe glass pane with a white ceramic print is predominantly diffuse

The light attenuation model needs to evaluate the angle-dependent light propagation at material interfaces and pathlength-dependent absorption within materials to describe light scattering of ceramic prints. The optical model described in the next section is capable of taking both effects into account.

3. MODELLING

3.1 Description of the optical model
The optical model used in this work is a simplified version of the matrix approach also applied in the OPTOS formalism [6, 7]. Unlike OPTOS, it takes multiple reflections only within one of the optically thick sheets into account and it is restricted to unpolarized light of one single wavelength. Within this method, the power distribution of light is described by vectors with finite elements corresponding to a number of discrete angle channels.

$$v_n = \begin{pmatrix} p(\vartheta_1) \\ \vdots \\ p(\vartheta_i) \\ \vdots \\ p(\vartheta_m) \end{pmatrix} \quad (1)$$

with
v_n = nth power distribution vector
$p(\vartheta_i)$ = power fraction for angle i
ϑ_i = polar angle between 0° and 90° in 1° steps

Refraction or scattering of light rays at material interfaces leads to a redistribution of power between angle channels and an angle-specific power loss. A redistribution matrix provides the information on power loss and redistribution. Surface interaction is efficiently modelled by multiplying the incoming power distribution vector with a redistribution matrix.

$$v_{out} = v_{in} \times TM_x \quad (2)$$

with
v_{out} = outgoing vector
v_{in} = incoming vector
TM_x = propagation or redistribution matrix for layer/interface x

The allocation of the output angle at an interface to the incoming angle within the redistribution matrix is computed with Snell's law while the power fraction transmitted or reflected for each angle channel is computed by Fresnel's law.

The Lambert-Beer law describes the exponential decay of the power of a light ray within homogeneous, absorbing material. Multiplying the power distribution vector of an incoming light ray with the propagation matrix TM_1 allows for accurate computation of the pathlength-dependent absorption within material layers.

$$TM_1 = \begin{pmatrix} e^{-\alpha d/\cos\vartheta_1} & \cdots & 0 \\ \vdots & \ddots & \vdots \\ 0 & \cdots & e^{-\alpha d/\cos\vartheta_m} \end{pmatrix} \quad (3)$$

with
α = absorption coefficient
d = glass thickness
ϑ_i = polar angle between 0° and 90°

The scattering print layer is made up of a glass matrix that contains scattering particles and pigments [5]. The print layer is described by a redistribution matrix that redistributes the incoming light intensity between angle channels. The scattering is assumed to be isotropic, however Nitz showed that prints can have an uneven scattering behavior comparing front and rear power distribution [8]. The ratio of reflected and transmitted light is influenced by layer thickness, scattering particle concentration and optical coupling. Therefore, we implemented an adjustable print transmittance factor that allows the forward and backward scattered power fractions to be varied.

As we expect the refractive index of the enamel glass matrix to be close to the refractive index of the glass substrate, we neglect transmittance losses at the glass/enamel interface. Due to the narrow layer thickness of the white enamel (5 µm) and no observed absorption minima in transmittance measurements (see Fig. 3), we assume the white print absorbance to be negligible. Therefore we assumed the absorbance to be zero in our model.

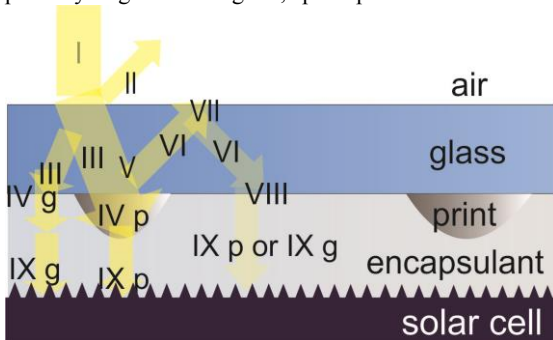3.2 Application of the model to a (printed) glass pane in air
The light attenuation is modelled by following the light path through the system as shown in Figure 4. The incoming light intensity is defined as 100%, normally incident radiation is assumed (1). The transmittance is calculated at the air/glass interface (2). The internal transmittance for the glass is calculated based on the path length (3). At the rear glass surface, the light intensity is weighted according to the coverage ratio. Light attenuation at the unprinted rear glass/air interface will be processed according to the Fresnel laws (4g). Multiple internal reflections starting from the unprinted rear interface is considered in the effective transmittance until the intensity of the reflected vector sinks below 0.01% of the incoming light intensity.

Light attenuation at the printed rear interface is calculated differently since scattering at the print occurs. The incoming light intensity is divided according to the print transmittance factor into a transmittance and a reflectance vector (T=1-R) labeled with 4p and 5 in Figure 4. The power distribution in both vectors is isotropically distributed into all angle channels.

This reflectance vector is the starting point of an iteration, calculating the transmittance due to multiple reflection within the printed glass pane: The reflectance vector is attenuated by the internal glass transmittance (6), glass/air reflectance (7) and again internal transmittance (6) before being weighted again by the coverage ratio and transmittance is computed for the respective interface labeled as 8g and 8p in Figure 4. Light ray (9) indicates the beginning of a new iteration in which steps (5) to (8) are repeated. Iterations are repeated until the remaining light intensity in the layer stack (9) sinks below 0.01%. After each iteration step, the sum of all light intensities 4g, 4p, 8p and 8g is calculated as the effective transmittance.
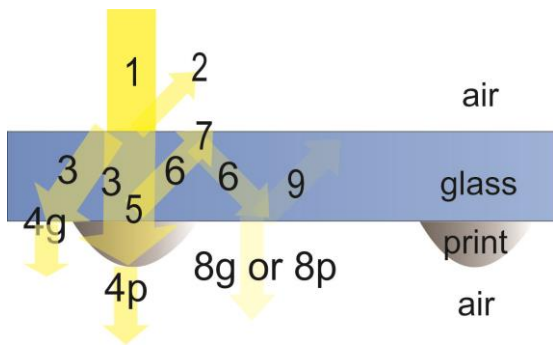
Figure 4: Glass pane in air with light attenuation pathways. "g" refers to glass, "p" to print.

Figure 5: Modelled 'laminated stack' with light attenuation pathways, solar cell is modelled as perfect transmitting and fully absorbing.

3.3 Application of the model to a simplified module stack with printed glass

The module is modelled in a similar way to the glass/encapsulant stack displayed above (Figure 5). The differences to the glass pane setup are:

- ☐ Due to optical coupling of the enamel with encapsulant, the transmittance of the rear print surface increases (IVp > 4p)
- ☐ Glass and the encapsulant have similar refractive indices, so the reflectance IVg and VIII at the unprinted rear glass/encapsulant interface is negligible.
- ☐ The solar cell is assumed to show no reflection at the front surface and perfect absorption in the bulk. This is a sufficient approximation for comparing different print coverages as done within this work, since the reflectance of a random pyramid interface with ARC is low [9].

4. RESULTS

4.1 Results - glass pane in air

To validate the model, we plot the relative, modelled normal-hemispherical transmittance over the relative, measured transmittance of a glass pane in air for coverage ratios 0% to 100% as shown in Figure 6. The print transmittance factor was used as fitting parameter being constant for all coverage ratios.

By definition, the relative normal-hemispherical transmittance of the reference glass pane (print coverage of zero) is set to 100%. For a print transmittance factor of 30%, we find very good correlation of the results for coverage ratios equal and below 98%.
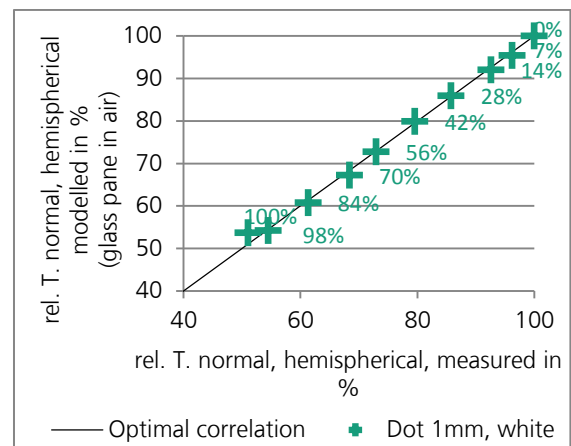
Figure 6: Correlation between computed and measured relative normal-hemispherical transmittance T. for a glass pane in air.

The deviation in the modelled transmittance for 100% can be explained by a different printing process with different droplet positioning of the inkjet leading to a thicker enamel layer and consequently to a lower measured transmittance [5]. In consequence the 100% value is not taken into account when the root mean square error (RMSE) values are calculated below.

4.2 Results - simplified module stack

Figure 7 shows the modelled normal-hemispherical transmittance within the laminated stack over the relative module power for coverage ratios 0 to 100% and a print transmittance factor of 68%. The print transmittance factor is constant for all coverage ratios, but is not equal to that determined from the printed glass panes. The optical coupling of the enamel with encapsulant leads to higher print transmittance.

For lower coverage ratios (14 to 28%) the modelled transmittance in the module stack slightly underestimates the actual transmittance, while for higher coverage ratios (98%) the modelled transmittance is slightly overestimated compared to the measured module power.

We do not consider the angle-dependent solar cell reflectance in our model. The observed deviation between modelled and measured data might be explained by this effect. We expect that with higher print coverage ratios, the share of diffuse light reaching the solar cell will also increase. The more light hits the solar cell at an oblique angle, the higher the solar cell reflectance is. As a result, the modelled transmittance is slightly overestimated for higher print coverage ratios.

At 100% coverage, the change in printing parameters is again assumed to be responsible for the discrepancy between the modelled and measured results.
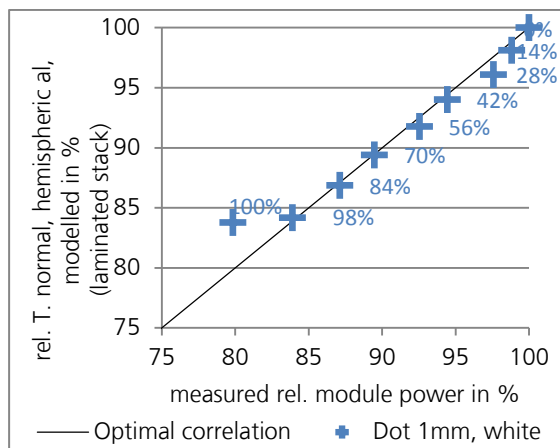
Figure 7: Correlation between modelled relative transmittance of the laminated stack and relative module power.

5   DISCUSSION

The good correlation of the modelled and measured transmittance of the glass pane in air demonstrates that the matrix model is capable of describing the correlation between coverage ratio and transmittance of light-scattering printed glass panes. A RMSE of 0.55% for coverage ratios from 0 to 98% is very low. Hereby, the print transmittance factor plays a key role as a fitting parameter, as it determines the ratio of transmitted and reflected light intensity by the print layer for a given background material.

Likewise, the overall correlation between modelled transmittance in the module stack and relative module power is good. A RMSE of 0.73% for 0 to 98% coverage is good.

By adjustment of the print coverage ratio and the print transmittance factor, modelling of various white prints is now possible. The linear correlation between the modelled and measured data sets indicates that all main optical influence factors are considered within the model.

6 CONCLUSIONS AND OUTLOOK

The introduced matrix model, based on a simplified OPTOS formalism, can accurately describe the transmittance of partially printed glass panes in air as well as the relative power loss of the corresponding module. The print transmittance factors, that determine the ratio of transmitted/reflected light power by the print layer, plays a key role. They are empirically determined by fitting the modelled data points to obtain the lowest RMSE to the measured transmittance data, for a series of partially printed glass panes, either in air or in the module configuration.

It should be possible to determine the print transmittance factor by detailed characterization of the ceramic print enamels, e.g. by determination of the bidirectional scattering distribution functions (BSDF). With this information, the module power could then be predicted by application of the described approach.

By modelling both configurations, the light attenuation processes within printed glass panes and modules are well explained. The optical coupling of the glass pane with encapsulant and thereby the inhibition of total internal reflection of the scattered light at the rear glass surface can be identified as the relevant difference between the two optical systems.

The model can be extended for colored prints by the implementation of an absorbance factor of the print layer.

REFERENCES

[1] L.H. Slooff, J.A.M. van Roosmalen, L.A.G. Okel, T. de Vries, T. Minderhoud, G. Gijzen, T. Sepers, A. Versluis, "An Architectual Approach For Improving Aesthetics Of PV," in *Proceedings of the 33rd European Photovoltaic Solar Energy Conference and Exhibition*, Amsterdam, 2017.

[2] P. Hannen, "Facade built with photovoltaic modules in six sizes and 7 print patterns," https://www.pv-magazine.de/2017/10/27/fassade-mitphotovoltaik-.

[3] F. Frontini, P. Bonomo, E. Saretta*, T. Weber, J. Berghold, "Indoor and Outdoor Characterization of Innovative Colored BIPV Modules for Façade Application," in *Proceedings of the 32nd European Photovoltaic Solar Energy Conference and Exhibition*, Munich, Germany, 2016, pp. 2498–2502.

[4] M. Mittag, C. Kutter, M. Ebert, H.R. Wilson, U. Eitner, "Power loss through decorative elements in the front glazing of BIPV modules," in *Proceedings of the 33rd European Photovoltaic Solar Energy Conference and Exhibition*, Amsterdam, 2017, pp. 2609–2613.

[5] H. R. Wilson and M. Elstner, "Spot Landing: Determining the Light and Solar Properties of Fritted and Coated Glass," in *Glass Conference Proceedings, Vol 6 (2018): Challenging Glass 6*, pp. 203–212.

[6] J. Eisenlohr *et al.,* "Matrix formalism for light propagation and absorption in thick textured optical sheets," (eng), *Optics Express*, vol. 23, no. 11, A502-18, 2015.

[7] N. Tucher *et al.,* "Optical simulation of photovoltaic modules with multiple textured interfaces using the matrix-based formalism OPTOS," (eng), *Optics Express*, vol. 24, no. 14, A1083-93, 2016.

[8] Dr. Peter Nitz, *Optische Modellierung und Vermessung thermotroper Systeme*. Inaugural-Dissertation. Freiburg im Breisgau, 1999.

[9] I. Geisemeyer *et al.,* "Angle Dependence of Solar Cells and Modules: The Role of Cell Texturization," *IEEE J. Photovoltaics*, vol. 7, no. 1, pp. 19–24, 2017.